AUT Journal of Electrical Engineering

AUT J. Electr. Eng., 56(2) (2024) 325-342
DOI: 10.22060/eej.2024.22866.5565

Providing a fault detection method for the occurrence of faults in DC microgrids, distributed generations, and electrical vehicles

Alireza Sistani[1], Seyed Amir Hosseini*[1], Vahideh Sadat Sadeghi[1], Behrooz Taheri[2]

[1] Electrical and Computer Engineering Group, Golpayegan College of Engineering, Isfahan University of Technology, Golpayegan, Iran
[2]Department of Electrical Engineering, Qazvin Branch, Islamic Azad University, Qazvin, Iran

ABSTRACT: DC microgrids have emerged as a promising solution to provide reliable and efficient power for various applications. However, similar to any power system, DC microgrids are prone to faults that can disrupt their performance. Accordingly, the lack of publication of sufficient standards and guidelines for the protection of DC microgrids makes it necessary to develop protection methods in these networks. Therefore, the purpose of this paper is to create a new fault detection method in islanded DC microgrids. In this method, the current signal samples are entered into a chaotic state, and using the feature of sensitivity to the initial conditions of this method, it accurately identifies the fault. In this case, the signal undergoes a very large chang during the fault, which is easily visible compared to the normal state. It should be noted that, unlike other methods, in the proposed method in this paper, only one measurement unit is used in the DC bus for sampling signals. Therefore, there is no need to use communication links in the proposed method. The proposed method has been implemented using MATLAB/Simulink software on a sample DC microgrid. The results show that the proposed method is capable to detect pole-to-pole and pole-to-ground faults on the microgrids and also faults on the distributed generations and electrical vehicles. Also, results prove that this method is resistant to the operational uncertainty of distributed generations, electrical vehicles, and the destructive effects of noise on the sampled signals.

Review History:

Received: Dec. 15, 2023
Revised: Jan. 18, 2024
Accepted: Jan. 22, 2024
Available Online: Mar. 01, 2024

Keywords:

DC Microgrid
Chaos Theory
Fault Detection
White Gaussian Noise
Uncertainty

1- Introduction

The concern about the increase of the Earth's heat due to the consumption of fossil fuels has increased the use of renewable energy resources [1]. Also, with the increasing number of DC loads such as computers and electrical vehicles (EVs), the traditional power grid is prone to become a modern system for energy supply [2]. For this purpose, the use of microgrids is increasing continuously. It should be mentioned that the collection of renewable energy resources, loads, and energy storage systems is called a microgrid [3].

Microgrids are divided into two AC and DC categories depending on their voltage type. With the advancement of power electronic devices and increasing DC loads, it is easier to use DC microgrids [4]. DC microgrids are known as a promising solution to provide reliable and efficient power for various applications [5]. DC microgrids have several advantages over AC type [6, 7]. However, similar to any power system, DC microgrids are prone to faults that can disrupt their performance [8]. In fact, in these microgrids, the short length of lines causes the low impedance of the lines and as a result, the current reaches its peak in a very short period of time [9]. This amount of current can cause serious damage to the power electronic devices [10]. Also, the lack of a natural zero point in the fault current challenges the process of detecting and clearing the fault in DC microgrids [11, 12]. It should be mentioned that the sensitivity of fault response is significantly influenced by fault resistance, as discussed in [13].

Another issue that can make fault detection in DC microgrids challenging is the transient states in DC microgrids [14]. Uncertainty in the amount of generation power in distributed generation (DG) units as well as disconnection and connection of loads causes this situation. Another transient mode that can disrupt the fault detection process in these microgrids is the effect of noise on the network signals [15]. This is despite the fact that some previous methods may have maloperation by considering the effects of noise in their fault detection methods. To investigate this problem, the method presented in [16] has been used. In the proposed method in [16], the fault is detected by sampling the current signal and then obtaining the specified index. In this case, if the obtained index exceeds a threshold value, it indicates a fault in the system. To investigate this method, the sampled signals were applied once without considering the noise and again by applying white Gaussian noise with a signal-to-noise ratio of (SNR)=30 dB to the algorithm presented in

*Corresponding author's email: s.hosseini@iut.ac.ir

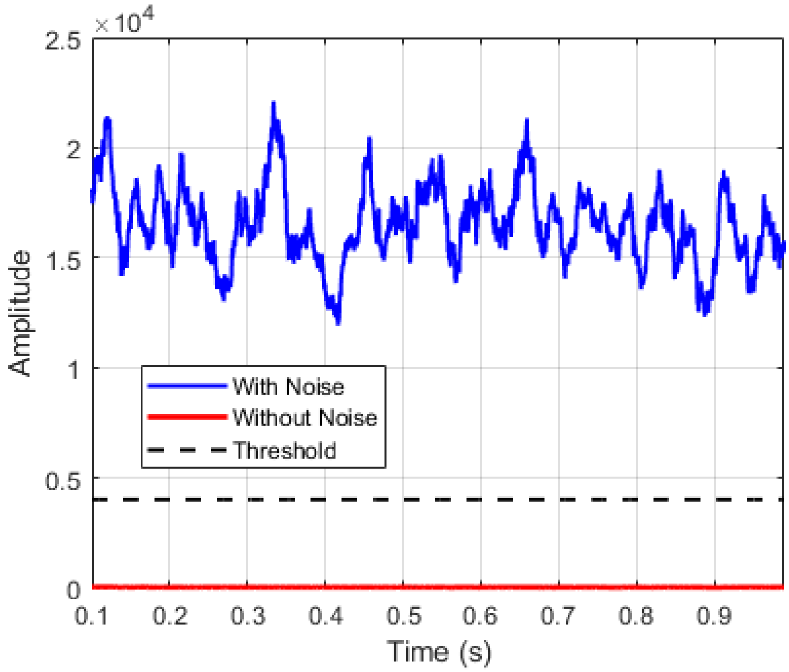

Fig. 1. Evaluation of the proposed method in [16] with/without considering the effect of noise

[16]. The results are presented in Fig. 1. As shown in this figure, when the noise has not affected the sampled signals, the algebraic sum of the sampled currents is equal to zero. Therefore, the network is in the normal mode. This is while, according to Fig. 1, when the effect of noise is applied to the current signals, the protection system has incorrectly detected a fault in the microgrid. Therefore, it is necessary to develop a fast and reliable method for detecting faults in DC microgrids considering the affecting uncertainties [9].

In recent years, the interest in conducting research in this field has led to the development of various methods. In this regard, methods such as the use of artificial intelligence, differential protection, voltage analysis, wavelet analysis, signal processing, and impedance estimation have been presented [3]. Accordingly, in [17-20] the differential protection method has been used. The method proposed in [9] has also used the logic of differential protection with the difference that in this study several intelligent electronic devices (IEDs) have been used. In a similar scheme, in [21], the difference between two consecutive samples of the current signal and comparison them with two fixed and adaptive threshold values are used for fault detection. Furthermore, the authors in [22, 23] have conducted an analysis of fault detection based on the difference in current signals sampled from the beginning and the end of the microgrid lines. Nevertheless, the method proposed in these studies only identified faults occurring in the main lines of the microgrid. Authors in [24] have used rapid changes in voltage and current signals using local measurements for fault detection. The authors in [25] have detected the fault by using the currents measured by IEDs and using a measurement index. In this study, only Pole-to-Ground (PG) faults have been detected. In [26], by sampling the current signal and sending data to a control unit through communication links, various types of faults have been detected. In the control unit, by using the derivation of currents at consecutive times and comparing them with the threshold value, if the changes exceed the threshold, a fault has been detected. Uncertainties in communication links as well as the problem of synchronizing data sent to the control unit are the problems of methods using these links [14]. Two steps are used for fault detection in [27]. In the first step, by measuring the derivative of the current at the beginning of the cable and comparing it with the pickup value, if it exceeds the threshold, the fault is detected. If the measured value is lower than the threshold value, it has been entered into the second step. In the second step, by measuring the derivative of the current at the end of the cable and comparing it with the current at the beginning of the cable, if the ratio becomes negative, the fault has been detected. In the method presented in [28], the voltage signal is used for fault detection. However, in the proposed method in [28], the type of occurred fault (PG or Pole-to-Pole (PP)) is not detected. To detect the fault, the authors in [29] have used a method based on measuring the current and comparing it with the state when the network is in a normal mode. In [30] resistance estimation has been used for fault detection in DC microgrids. This method has been implemented in two stages. In the first stage, by sampling the current signal, the derivative of the current is compared with a threshold value. In the second step, the resistance between the voltage source and the desired bus is estimated by IEDs placed at the beginning and end of each line. Accordingly, if

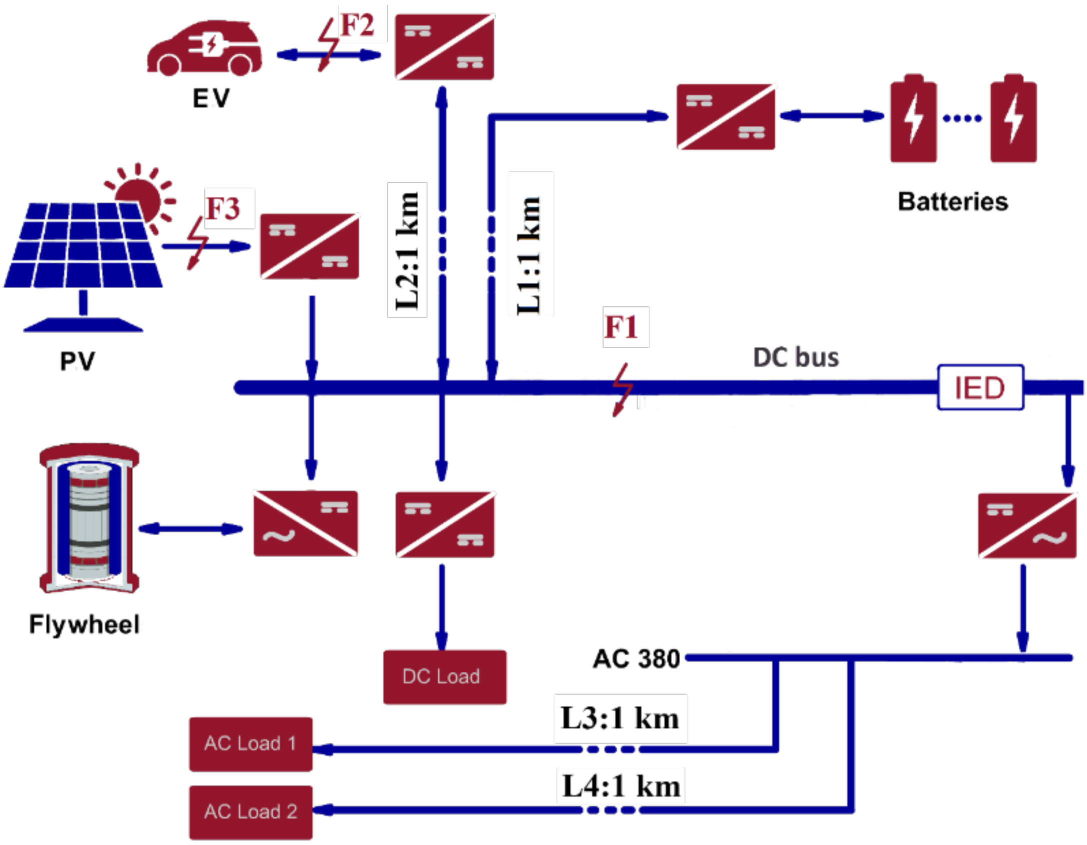

Fig. 2. Sample DC microgrid structure

the estimated resistance is negative, occurred fault has been detected. In [31], traveling waves are used for fault detection. However, the performance of this method may be impaired when the fault occurs near the measurement devices. Another widely employed method for protecting DC microgrids is overcurrent protection. This method involves dividing the microgrid into several zones and deploying corresponding relays within these zones to detect faults, as explained in [32].

Failure to consider transient states in microgrids as well as the effects of noise on the sampled signals are problems of the previous studies. Therefore, in this paper, a new method for fault detection in DC microgrids is proposed. In the proposed method, the chaos theory of logistic map type has been used for fault detection [33, 34]. In order to eliminate the operational uncertainties of the communications links in the proposed method, in this method, local data is used for fault detection. Therefore, to realize this method, only an IED is installed at the DC bus, and based on the local current calculation, it detects the fault on the islanded microgrid. To detect the fault, the current signal sampled by the IED enters the proposed chaotic state. In this case, the signal undergoes very large changes during the fault, which is easily visible compared to the normal state. Therefore, if the signal entered into the chaotic state exceeds the predetermined threshold value, it indicates the occurrence of a fault in the DC microgrid. To evaluate the proposed method, this method is implemented on a sample microgrid using MATLAB/Simulink software. The results prove that the proposed method is capable of detecting types of faults in the DC microgrid and even in DGs. Also, the presence of transient disturbances, including white Gaussian noise, as well as uncertainties in the generation of DGs/EVs, do not affect the accuracy of the proposed fault detection method.

The structure of the paper is organized as follows. In Section 2, the sample DC microgrid is introduced. In Section 3, the proposed method for fault detection is described. In Section 4, the proposed scheme is tested on the sample DC microgrid and the results are analyzed during the occurrence of various faults and uncertainties. In Section 5, the proposed method is compared with previous studies, and its advantages are described.

2- Sample DC Microgrid

The sample DC microgrid used in this paper is shown in Fig. 2. This network is composed of a photovoltaic (PV) cell, an EV, hybrid energy storage systems (Battery and Flywheel), AC/DC converters, DC/DC converters, and AC and DC loads. The DC bus voltage in this network is 600 V and the AC voltage is 380 V. All devices in the microgrid are connected to the DC bus by power electronic converters.

Table 1. Sample DC microgrid parameters

Parameter	Value	Units
DC Bus Voltage	600	V
AC Voltage	380	V
PV Power	20	kW
EVs Charge & Discharge	15, 10	A
Battery	LiFePO4, 360, 100	V, Ah
Flywheel	10, 10000, 5000	kW, r/min, r/min
AC Loads	5	kW
DC Load	5	kW
Cross Section Area	240	mm^2
Cable Resistance	0.125	Ω/km
Cable Inductance	0.232	mH/km
Length of lines 1-4	1	km

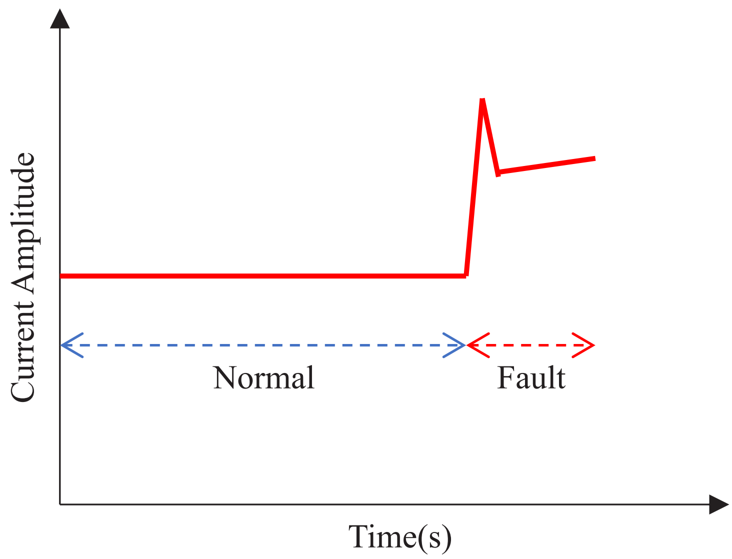

Fig. 3. An example of current sampled by IEDs during a fault

Because of the uncertainty of the generation of PVs and EVs, hybrid energy storage devices such as batteries and flywheels have been used to control their generation and optimize energy in this microgrid [35].

The sample microgrid includes 4 lines, L1-L4. The cross-section of each line is 240 mm^2. Aluminum cables with PVC type A insulation and PVC sheath type ST-1 are used in all lines [36]. Other information about this microgrid is presented in Table 1 [37, 38].

3- Proposed Method

3- 1- New fault detection method

The purpose of this paper is to present a suitable method for detecting the occurrence of different faults in DC microgrids. In general, during a fault in a DC microgrid, the current signal may be affected by different changes and disturbances. These changes can show themselves by increasing or decreasing the current. Figure 3 shows an example of a current signal variation during a fault. According to Fig. 3, when a fault occurs in the DC microgrid, the amplitude of the current signal has been suddenly increased. Accordingly, one of the criteria for detecting faults in DC microgrids is sudden changes in the current signal. However, due to the uncertainty in the topology of the microgrid and the amount of generation of DG units in DC microgrids, changes in the current signal at the time of the fault are not always constant. Therefore, there is a need to use a method that can highlight these changes and distinguish them from normal network conditions. For this reason, in this paper, chaos theory is used for fault detection.

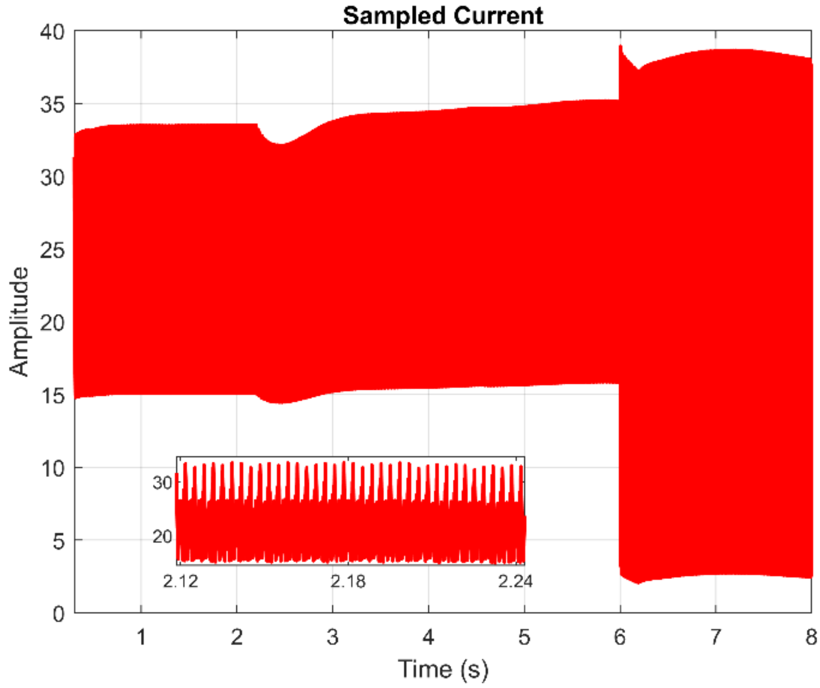

Fig. 4. Variations in the current amplitude when a fault occurs

Chaos theory is one of the mathematical theories that deals with the analysis of complex and non-linear systems [39]. This theory has features such as unpredictability and sensitivity to initial conditions over time. The sensitivity of this theory is such that if a small change occurs in the initial conditions of the system, the output of the system suddenly undergoes very large changes [40]. Considering this feature, analyzing signals in a chaotic environment can be a suitable method for detecting faults in the system [39]. A logistic map is one of the simple modes of chaos theory. This simple mathematical model is used to examine some problems of chaos theory such as chaos-based cryptography [41]. The proposed method for fault detection in this paper is based on chaos theory and its logistic map type.

To implement the proposed method, it is necessary to sample the current signals in the network. As shown in Fig2 ., this is done by installing only one IED on the sample microgrid DC bus. It should be noted that in the method proposed in this paper, the values measured by the IED do not need to be transmitted through communication links. Figure 3 shows an example of the current sampled by the IED unit when a fault occurs in one of the microgrid lines. As it is clear from Fig. 4, the waveform of the current signal has suddenly changed, which can indicate the occurrence of a fault in the microgrid. The oscillations depicted in this figure are attributed to the non-ideal modeling of converters. Therefore, to confirm the occurrence of the fault, the sampled signal is entered into the chaotic environment. Generally, to highlight the changes in the current signal over time and, as a result, the speed of action in fault detection, the sampled signals are analyzed by chaos theory [42].

To start the fault detection process in the DC microgrid by chaos theory, first, the sampled current signal is passed through a low pass filter. The reason for this is that different frequencies created by the chargeable power of energy storage sources, i.e., flywheel and battery, are separated by the filter. To implement the proposed method based on the logistic map model and to highlight the changes in the current signal, the sampled signal according to Eq. (1) has entered into a chaotic environment.

$$Z_{n+1} = f(Z_n) = \lambda Z_n (1 - Z_n) \tag{1}$$

where Z_n is the state variable of the n-th sample and λ is the system parameter. This parameter (λ) can be a number between 1 and 4 [43]. In this paper, based on the simulations, the value of one is considered.

To implement the proposed method, a window is required for sampling the current signal. To calculate the sampling window length, the sampling frequency is required. The sampling frequency in this paper is 250 kHz. Therefore, the length of the sampling window is equal to 5000 according to the sampling frequency and based on the method used in [43]. The obtained window length is applied to the sampled current signal. Therefore, the size of the sampled current signal has been changed according to Eq. (2) to a signal with the length of the data window.

$$Y = [y_1, y_2, \ldots, y_i] \tag{2}$$

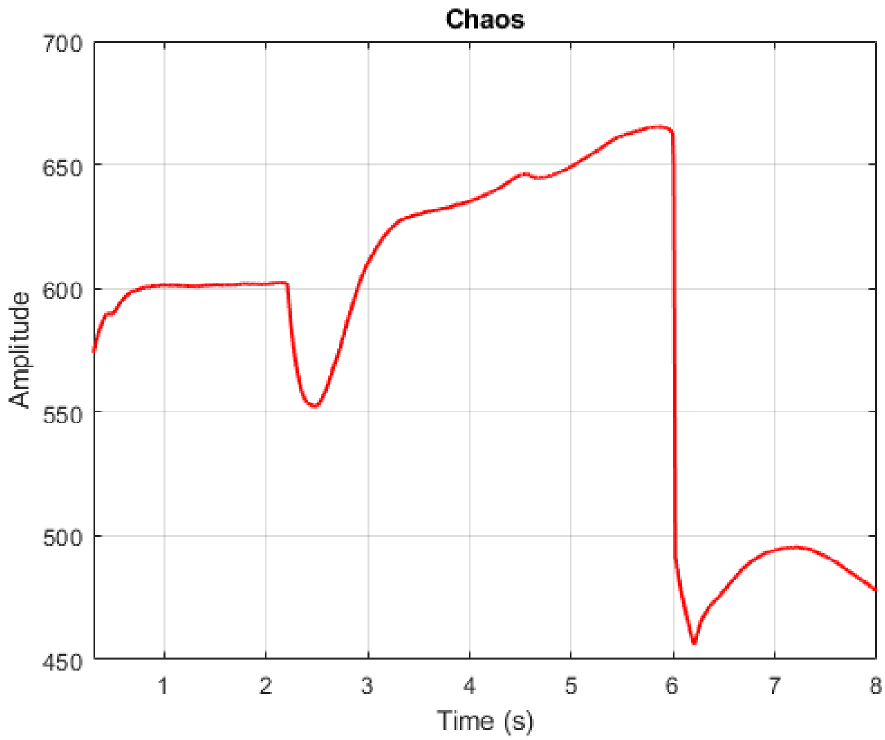

Fig. 5. Fault current amplitude with chaos theory

where Y is the matrix obtained from the sampled data and y_i is the *i*-th transformed signal as the window data.

Data in the Y matrix has entered into a chaotic state according to Eq. 1. Due to the nature of chaos theory, a small change in the input signal causes a large change in the output waveform. This feature can be used for fault detection. Therefore, Fig. 5 shows the sampled current signal (Fig. 4), which has entered into a chaotic state. As it is clear from Fig. 5, with the occurrence of small changes in the input of the system, due to entering into the chaotic environment, the output has suddenly undergone a large change in its amplitude.

It should be mentioned that DC microgrids have internal harmonics. This problem is due to the disturbance in the waveform of the sampled signal due to the switching of power electronics devices. Therefore, by taking RMS from the signal, the generated signal becomes free of fluctuations [44]. For this reason, using Eq. (3), the RMS of the current signal along the data window has been obtained [43].

$$RMS = \sqrt{\frac{\sum_{k=1}^{N} I^2}{N}} \tag{3}$$

Finally, the output of Eq. 3 is used to detect the fault in the DC microgrid. Accordingly, if the RMS of the current changes obtained using the proposed method is outside the threshold range, it indicates the occurrence of a fault in the microgrid. Therefore, the fault detection condition in the proposed method is presented in Eq. (4).

$$if\,(RMS < K_1 \quad or \quad RMS > K_2\,) \Rightarrow Fault\ det\,ected \tag{4}$$

In this equation, K_1 and K_2 are threshold values.

In general, Fig.6 shows the proposed fault detection process. As it is clear from this figure, the sampled data is first passed through a low-pass filter and then entered into a chaotic state by logistic map equations. Then, the signal entered into the chaotic environment has been compared with the threshold values to investigate the occurrence of a fault in the microgrid. If it has not violated the threshold, it has re-entered the first stage and started sampling the signals. On the other hand, if the obtained values exceed the fault detection threshold values, it indicates the occurrence of a fault in the microgrid and causes a trip command to be issued.

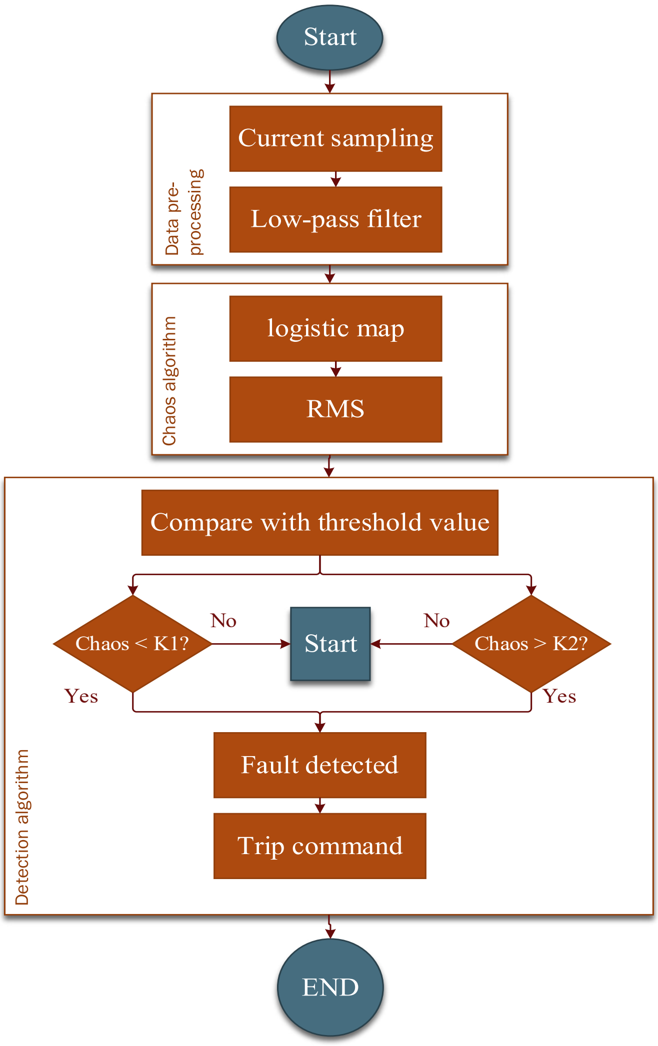

Fig. 6. The algorithm of the proposed method

3- 2- Calculation of the threshold values

In this study, numerical simulation is used to obtain the threshold values [45]. Therefore, considering that the proposed method in this paper has the ability to identify faults in both DGs and DC microgrids (in the DC bus or DC line), it is necessary to evaluate the occurrence of faults in all these locations. In normal conditions, DG resources such as EVs and PVs inject power into the microgrid and the direction of this power is towards the microgrid. At the time of occurring a fault in a DG unit, all these currents flow in the fault direction, so the amplitude of current at the IED location is reduced. This issue is illustrated in Fig. 7-a (F1 fault occurs on the DC bus) and Fig. 7-b (F2 fault occurs at the end of the L2 line and in the EV). On the other hand, similar to what is shown in Fig. 7-c (F3 fault occurs at the PV connected to the DC bus), when the fault occurs in the microgrid, the amplitude of the current measured by the IED is increased.

In order to obtain the highest and lowest threshold values, the effect of noise and generation uncertainties must be considered in the measured currents. For this purpose, by placing different types of faults with different impedances and also in different places (according to Table 2) in the sample microgrid in Fig. 2, the current values have been measured in all the studied cases. The measured currents were compared with each other and the lowest and highest currents obtained from all the study cases presented in Table 2 were selected. These values are shown in Table 3. According to this table, the minimum value of the fault current is 572.4 A, and the maximum fault current is 641.5 A. Therefore, considering a tolerance, the threshold values of K_1 and K_2 have been determined as 560 and 680, respectively.

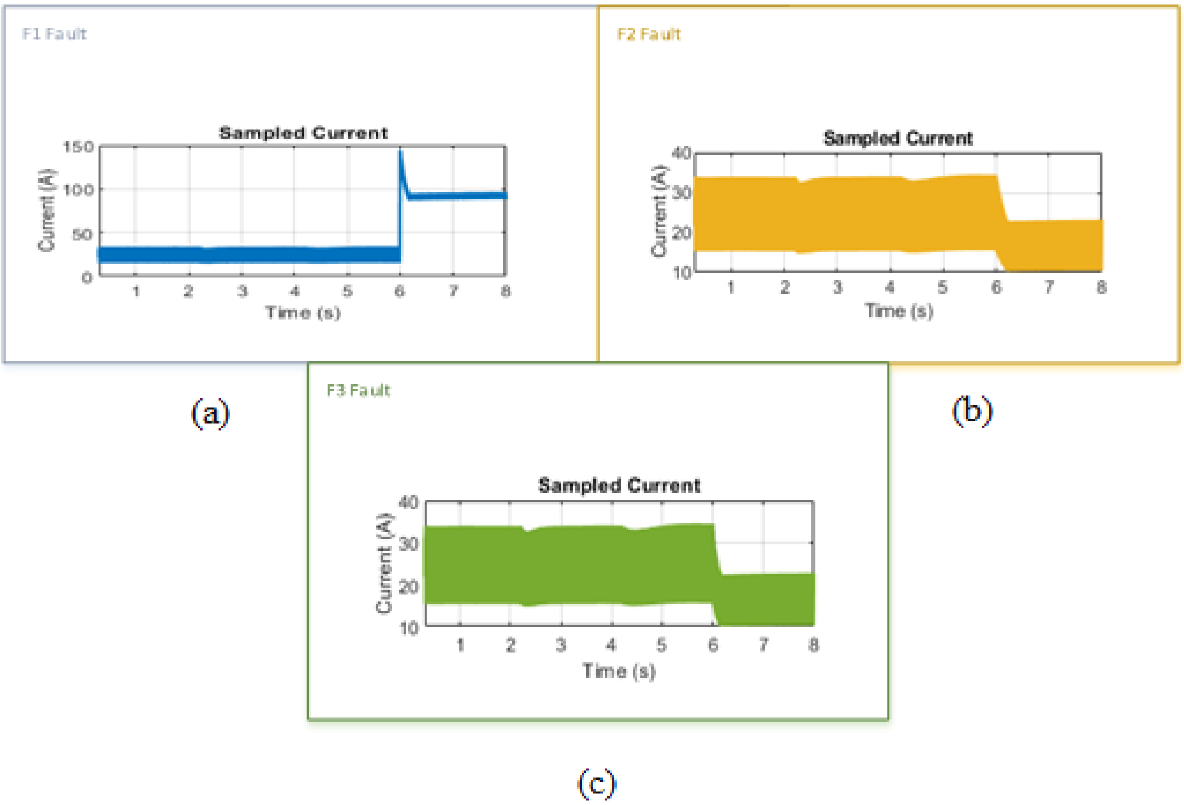

Fig. 7. Sampled currents during faults in different locations, a) a fault in the DC bus (F1), b) a fault in the EV (F2), c) a fault in the PV (F3)

Table 2. Analysis of different faults to determine threshold values

Case Study	Fault Location	Fault Type	Fault Impedance (ohm)	Distance between the IED and fault location (km)
1	F1	PG	1.5	0
2	F1	PP	1.5	0
3	F2	PG	1.5	1
4	F2	PP	1.5	1
5	F3	PG	1.5	1
6	F3	PP	1.5	1
7	F1	PG	2.5	0
8	F1	PP	2.5	0
9	F2	PG	2.5	1
10	F2	PP	2.5	1
11	F3	PG	2.5	1
12	F3	PP	2.5	1
13	F1	PG	5	0
14	F1	PP	5	0
15	F2	PG	5	1
16	F2	PP	5	1
17	F3	PG	5	1
18	F3	PP	5	1
19	F1	PG	10	0
20	F1	PP	10	0
21	F2	PG	10	1
22	F2	PP	10	1
23	F3	PG	10	1
24	F3	PP	10	1

Table 3. The Minimum and maximum amplitude of currents in different analyses of Table 2 (Amper)

Case Study	Min Current Amplitude	Max Current Amplitude
1-24	572.4	641.5

Table 4. The amplitude of the current (Amper) after the occurrence of various PG faults

Fault Location	$R_f = 1.50\Omega$	$R_f = 2.50\Omega$	$R_f = 5\Omega$	$R_f = 10\Omega$	$R_f = 15\Omega$	$R_f = 20\Omega$
F1	2712	2307	1741	1289	1097	991.7
F2	443.9	454.3	481.5	524.4	(Fault in F1)	(Fault in F1)
F3	72.7	82.1	158.1	273.9		

Table 5. The amplitude of fault currents (Amper) after the occurrence of various types of PP faults in the sample microgrid

Fault Location	$R_f = 1.50\Omega$	$R_f = 2.50\Omega$	$R_f = 5\Omega$	$R_f = 10\Omega$
F1	39890	17890	6529	6529
F2	264.2	274.9	421.7	421.7
F3	247.9	261.3	352	352

4- Simulation Results

To evaluate the efficiency of the proposed method, this method has been implemented on the sample microgrid in Fig2 .. It should be noted that MATLAB/Simulink software was used to implement the proposed method.

4- 1- Pole-to-Ground Fault

In order to evaluate the proposed method in PG fault detection, F1, F2, and F3 faults have been applied at the end of the DC bus, in EV (at the end of the L2 line), and in PV respectively at time t=6 s. In Table 4, the peak current amplitude after the occurrence of various types of PG faults with impedances of 1.5, 2.5, 5, 10, 15, and 20 ohms is presented. Also, the current signal waveforms obtained from all types of PG faults using the proposed method are shown in Fig. 8. Accordingly, Fig. 8-a shows the current signals when a PG fault has occurred in F1. As it is clear from this figure, in all investigated faults, the current signal sampled at the moment of the fault has crossed the upper threshold value (K_2). Therefore, the occurred faults have been correctly detected using the proposed method.

Fig. 8-b and Fig. 8-c show the state of the sampled signals when F2 and F3 faults occur, respectively. As it is clear, these signals have gone below the low threshold level (K_1) of fault detection. Therefore, it is clear that the detection of PG faults using the proposed method has been done correctly. It should be noted that the fault detection time using the proposed method is about 3 ms.

4- 2- Pole-to-Pole Fault

In the second case, the performance of the proposed algorithm during PP faults is investigated. Similar to the previous case, in this case, different PP faults including F1, F2, and F3 have been applied in the sample microgrid in Fig. 2 at t = 6 s. Table 5 shows the peak current after the occurrence of various types of PP faults with impedances of 1.5, 2.5, 5, and 10 ohms in all the studied cases. The obtained current signals using the proposed algorithm are shown in Fig. 9. According to Fig. 9, at t = 6 s when the PP faults occur (F1/F2/F3) with different impedances, the sampled current signals exceed the fault detection thresholds. These states indicate the occurrence of the faults (F1/F2/F3) at this time. It should also be noted that the time to detect all types of PP faults is about 3 ms.

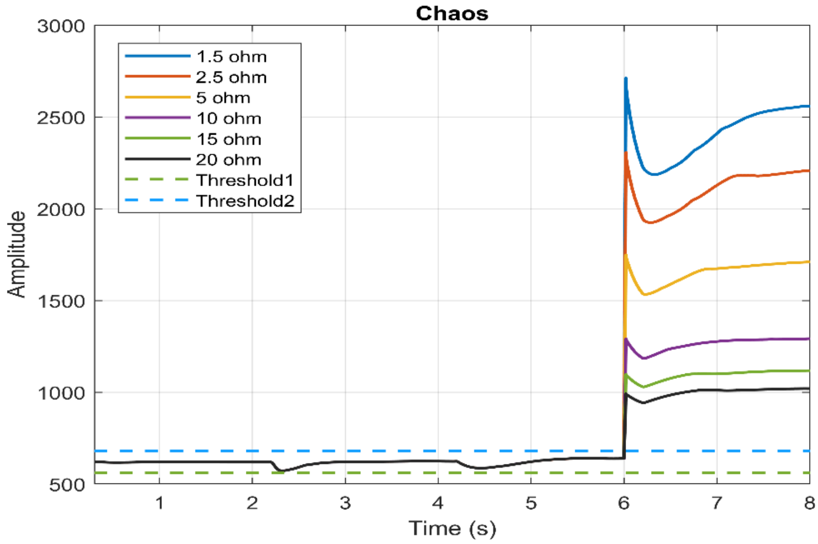

(a)

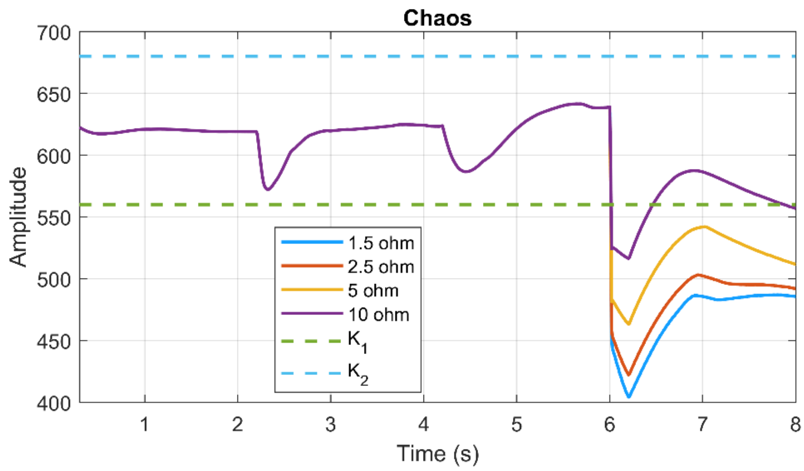

(b)

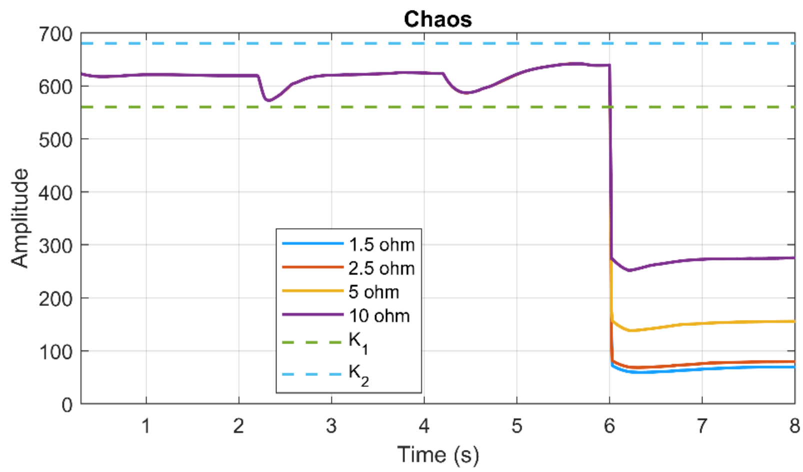

(c)

Fig. 8. Signals generated by the proposed algorithm for PG faults in a) F1 fault, b) F2 fault, c) F3 fault (Fig. 2)

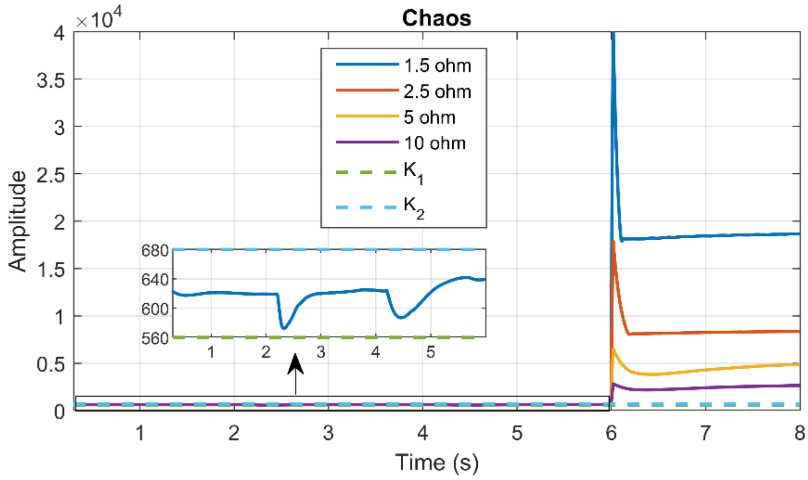

(a)

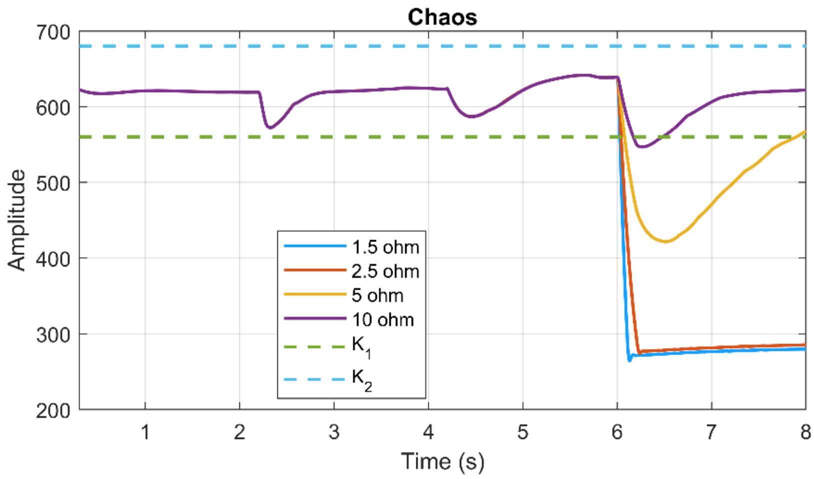

(b)

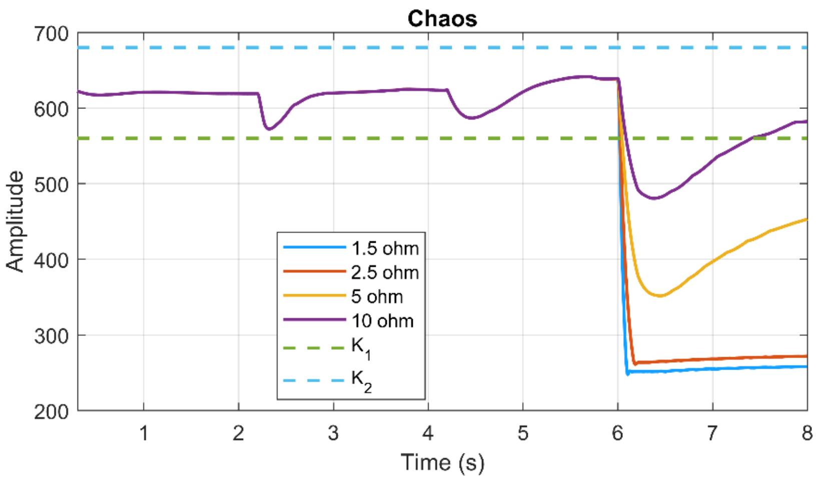

(c)

Fig. 9. Signals generated by the proposed algorithm for PP faults in a) F1 fault, b) F2 fault, c) F3 fault (Fig. 2)

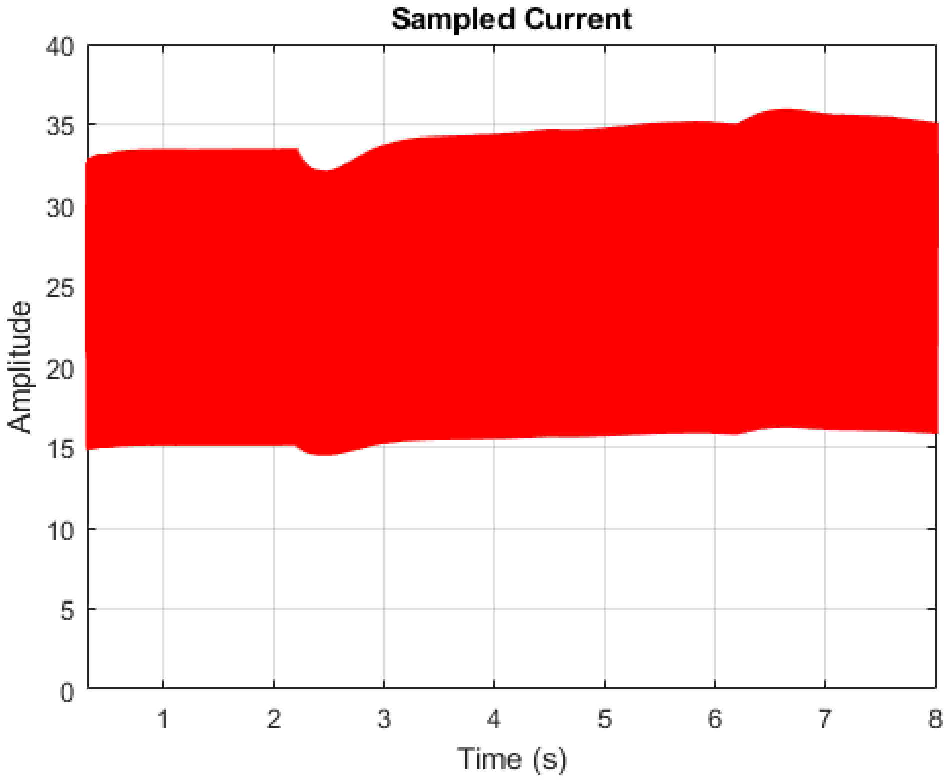

Fig. 10. Current signal recorded by the IED during transient conditions

4- 3- Transient Mode

Transient states may disturb the performance of the proposed fault detection algorithm. In fact, the proposed fault detection algorithm should be able to detect all the faults that have occurred and not perform against the transient states that occur in the network. This issue is evaluated in this section. Accordingly, first, at t = 0.2 s, all AC loads are in the network. EV is being charged and the generation is done by the PV. In this case, the surplus power generated by the PV is stored in the battery and causes the current to increase slowly. Then, at t=2.2 s, the PV generation power is suddenly reduced, and the lack of power must be compensated by the battery and flywheel. In this case, at first, the current of the DC bus is suddenly decreased, and then the current is increased with the help of compensators. Also, at the moment t=4.2 s, the DC load has entered the circuit, which causes the power to increase suddenly.

Figure 10 shows the current signal recorded by the IED during transient conditions. As it is clear from this figure, for all the applied changes, the transient fluctuations in the current signal are recorded. The signal recorded in Fig. 10 is entered into the proposed algorithm. Figure 11 shows the signal produced by this algorithm. As it is obvious, the proposed method was immune to the transient conditions of the network and correctly did not perform.

4- 4- Noise

In this section, the performance of the proposed method against Gaussian white noise with different SNRs such as 15 dB, 20 dB, 25 dB, and 30 dB is examined. To investigate this case, PG and PP faults are placed at the F1-F3 locations with 10 ohms in the sample microgrid in Fig. 2. In addition, the noise effect has been applied to the sampled current signals. Figure 12 shows the current signal sampled in the presence of noise. As it is clear from Fig. 12-a, b, c, and e, by applying PG and PP faults, the current amplitude has exceeded the fault detection threshold values, and therefore these faults have

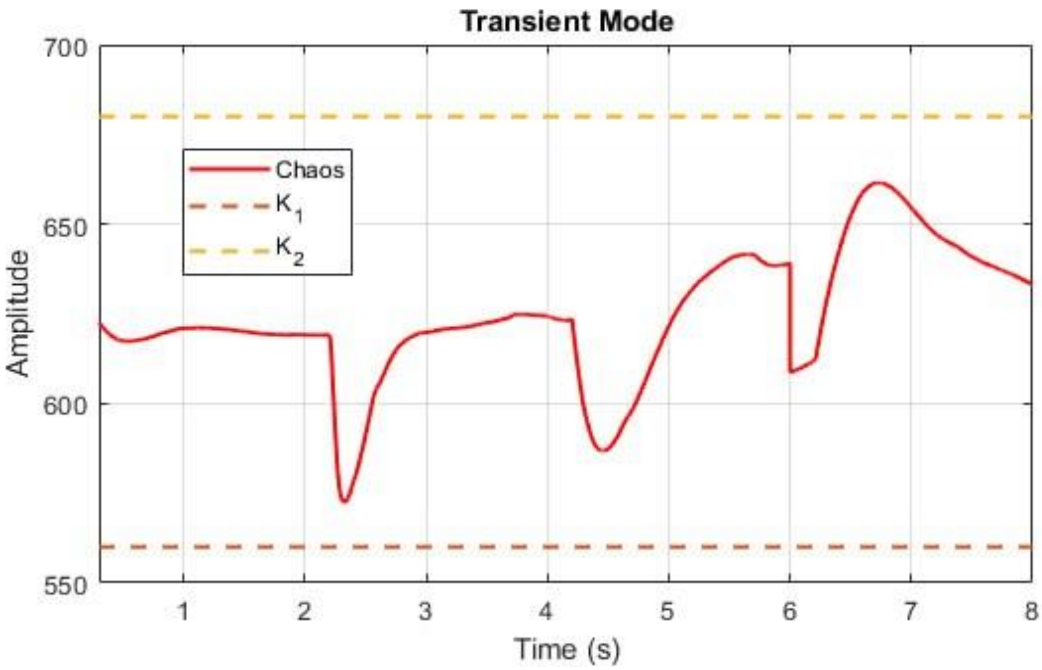

Fig. 11. The signal generated by the proposed algorithm in response to transient states

been correctly detected.

It should be noted that several different noise simulations with varying SNRs have been conducted. Figure 12 displays the results of these simulations. As evident from these findings, the proposed method encounters challenges when subjected to noise with an SNR of 15 dB, exhibiting incorrect performance.

Comparison of the proposed method with the previous studies

Table 6 compares the proposed method in this paper with the methods presented in previous studies. As it is obvious, the proposed method in this paper has a higher sampling frequency than all the studies compared in Table 6. Although this issue increases the reliability of the proposed method, it also increases the number of samples to be analyzed in the proposed method. However, the fault detection time in the proposed method is still within the framework of previous studies.

Another advantage of the proposed method compared to some previous studies is the use of local data for fault detection. Also, in all of the studies compared in Table 6, the effect of charging and discharging EVs is not considered. On the other hand, previous studies have focused only on fault detection in DC microgrids. However, the proposed method in this paper has the ability to detect faults in PV and EV. Therefore, it is clear that the method proposed in this paper can be a complete method for detecting all types of faults in DC microgrids, taking into account the effects of noise and generation uncertainties of DGs. It should be noted that the control system presented in [35, 38] operates at 250 kHz. Consequently, the sampling rate of the protection system is also set at the same value to ensure the consideration of the impact of all events created by the control system in the microgrid. Nevertheless, the proposed protection system retains the ability to operate with a lower sampling rate. Figure 13 illustrates the performance of the proposed method

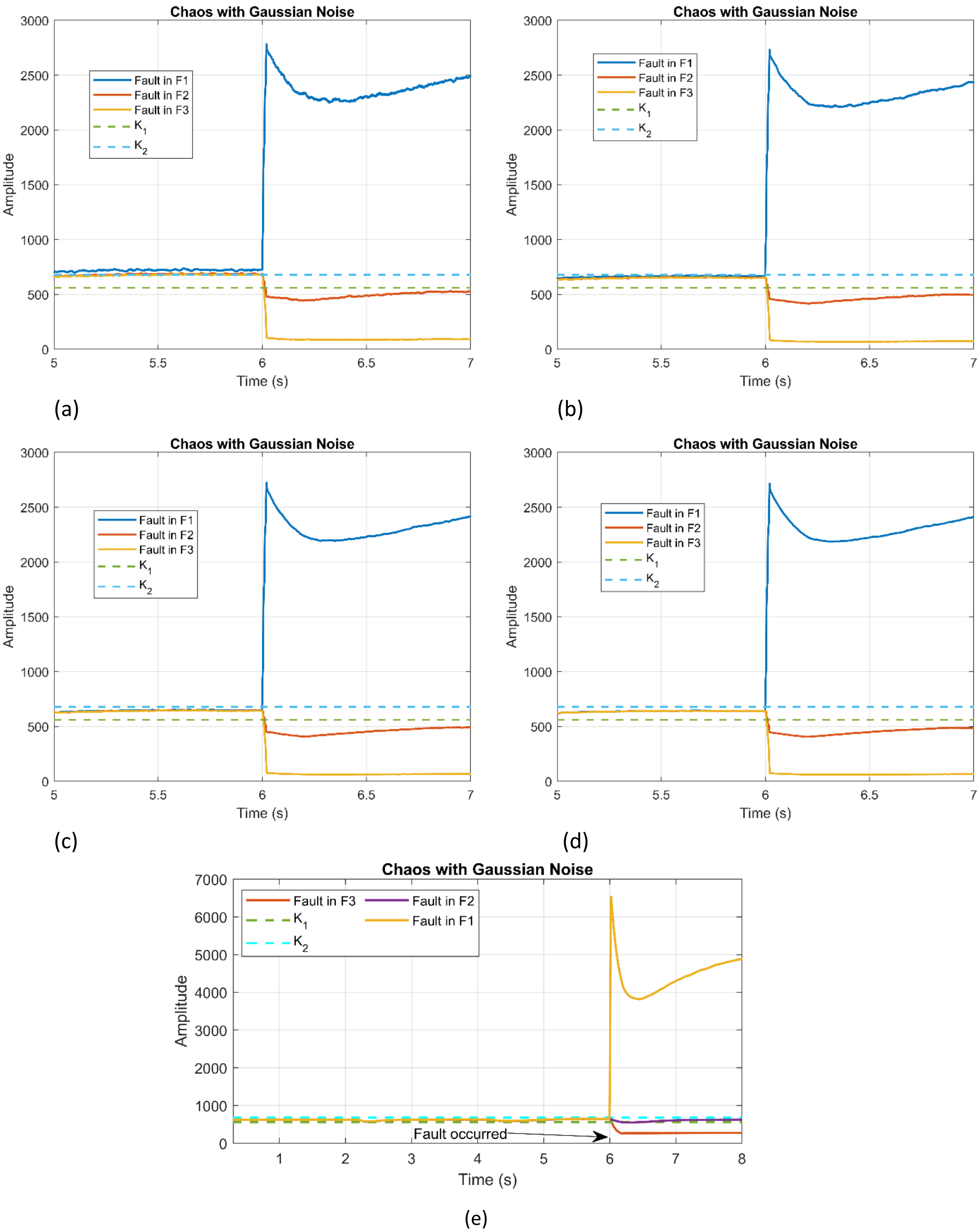

Fig. 12. Current signal recorded by the IED in the presence of white Gaussian noise, a) PG faults with SNR = 15dB, b) PG faults with SNR = 20dB, c) PG faults with SNR = 25dB, d) PG faults with SNR = 30dB, e) PP faults with SNR = 30dB

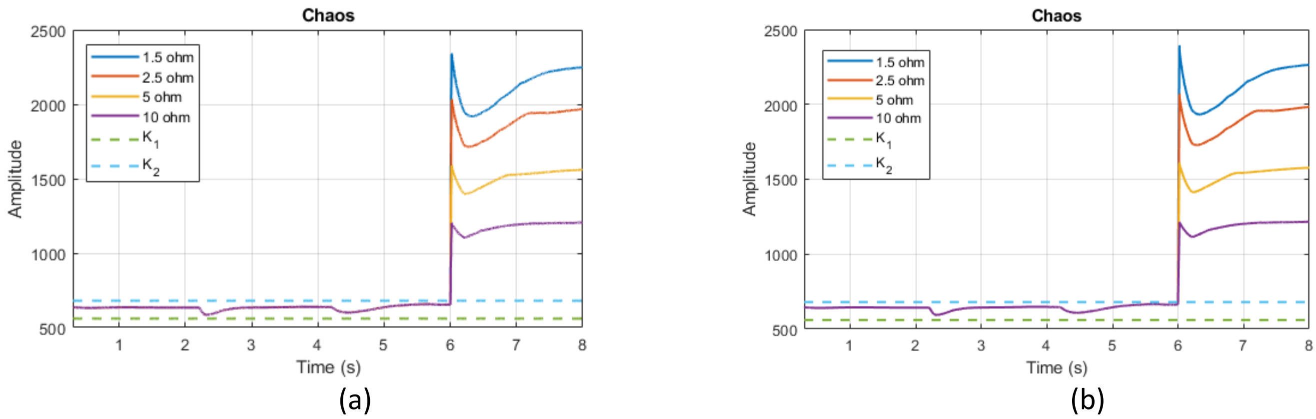

Fig. 13. Performance of the proposed method at sampling rates, a) 1 kHz and b) 10 kHz

Table 6. Comparison of the proposed method with other studies

Reference	Method	Sampling rate	Fault detection time in DC microgrid	Fault detection in PV and EV	Considering noise	Energy Storage	EV	PV	communication links	Threshold value determination
[46]	H∞/H−/regional pole placement	-	590 ms	×	✓	×	×	×	✓	✓
[47]	Current Assisted VMD based	10.025 kHz	3.95 ms	×	✓	Fuel cell & Battery	×	✓	✓	✓
[25]	Centralized Protection	4 kHz	3 ms	×	✓	Battery	×	✓	✓	✓
[48]	Local Measurement	20 kHz	0.2 ms	×	×	Battery	×	✓	×	✓
[29]	Pearson Correlation Coefficient	0.5, 1, 2, 5, 10 kHz	5 ms	×	×	×	×	✓	×	✓
[9]	Modified squared poverty gap index	5 kHz	1.2 ms	×	✓	Fuel cell & Battery	×	✓	✓	✓
[49]	Measuring Current & Voltage	2, 4, 8 kHz	1.25 ms	×	✓	Battery	×	✓	×	✓
[50]	Centralized Protection	-	4.2 ms	×	×	×	×	×	✓	✓
[51]	Differential Protection Strategy	5 kHz	100 ms	×	✓	×	×	✓	✓	✓
[24]	Local Measurement	-	<1ms	×	×	×	×	×	✓	✓
Current paper	Chaos Theory	250 kHz	3 ms	✓	✓	Battery & Flywheel	✓	✓	×	✓

at sampling rates of 1 kHz and 10 kHz.

5- Conclusion

Any scheme presented for fault detection in DC microgrids must be able to perform correctly when faults occur in these networks, taking into account the transient states in the network as well as the effect of noise. To realize this problem, a new method for fault detection in DC microgrids using chaos theory is presented in this paper. The fault detection method proposed in this paper performs the fault detection process with high accuracy by sampling the current signal by only one IED. The sampled current signals are first entered into the chaotic environment by chaos theory and then analyzed. The main feature of this method is its sensitivity to small changes in initial conditions. Accordingly, if there is a small change in the sampled current signal, the amplitude of the output signal will change a lot. The results of implementing the proposed method on a sample microgrid show that this method can detect all types of PG and PP faults with different impedances and in different locations (in DC microgrid, PV, and EV). Also, the implementation of the proposed method by considering the transient states in the microgrid and considering the effect of noise, shows that this method is capable of detecting faults in DC microgrids in the presence of these uncertainties. Therefore, according to the correct performance of the proposed method in different modes, this method can be implemented on any microgrid. To advance research in the field of DC microgrid protection, researchers can explore areas such as high-impedance fault detection (fault impedance above 100 ohms) and fault location in DC microgrids. Additionally, the complete elimination of the threshold value, considering the impact of noise in DC microgrids, remains a fundamental challenge and could serve as a promising avenue for future studies.

References

[1] J.J. Justo, F. Mwasilu, J. Lee, J.-W. Jung, AC-microgrids versus DC-microgrids with distributed energy resources: A review, Renewable and Sustainable Energy Reviews, 24 (2013) 387-405.

[2] W. Javed, D. Chen, Low voltage DC microgrid protection system-A review, in: 2018 53rd International Universities Power Engineering Conference (UPEC), IEEE, 2018, pp. 1-6.

[3] V. Terzija, G. Valverde, D. Cai, P. Regulski, V. Madani, J. Fitch, S. Skok, M.M. Begovic, A. Phadke, Wide-Area Monitoring, Protection, and Control of Future Electric Power Networks, Proceedings of the IEEE, 99(1) (2010) 80-93.

[4] M. Starke, L.M. Tolbert, B. Ozpineci, AC vs. DC distribution: A loss comparison, in: 2008 IEEE/PES Transmission and Distribution Conference and Exposition, IEEE, 2008, pp. 1-7.

[5] S.A. Hosseini, B. Taheri, S.H.H. Sadeghi, A. Nasiri, An Overview of DC Microgrid Protection Schemes and the Factors Involved, Electric Power Components and Systems, (2023) 1-31.

[6] D. Salomonsson, L. Soder, A. Sannino, Protection of low-voltage DC microgrids, IEEE Transactions on Power Delivery, 24(3) (2009) 1045-1053.

[7] S.-A. Amamra, H. Ahmed, R.A. El-Sehiemy, Firefly algorithm optimized robust protection scheme for DC microgrid, Electric Power Components and Systems, 45(10) (2017) 1141-1151.

[8] L. Tao, C. Schwaegerl, S. Narayanan, J.H. Zhang, From laboratory Microgrid to real markets—Challenges and opportunities, in: 8th International Conference on Power Electronics-ECCE Asia, IEEE, 2011, pp. 264-271.

[9] M. Salehi, S.A. Taher, I. Sadeghkhani, M. Shahidehpour, A Poverty Severity Index-Based Protection Strategy for Ring-Bus Low-Voltage DC Microgrids, IEEE Transactions on Smart Grid, 10(6) (2019) 6860-6869.

[10] N. Bayati, A. Hajizadeh, M. Soltani, Protection in DC microgrids: a comparative review, IET Smart Grid, 1(3) (2018) 66-75.

[11] S. Mirsaeidi, X. Dong, S. Shi, B. Wang, AC and DC microgrids: A review on protection issues and approaches, Journal of Electrical Engineering and Technology, 12(6) (2017) 2089-2098.

[12] R. Rahmani, S.H.H. Sadeghi, H. Askarian-Abyaneh, M.J. Emadi, An entropy-based scheme for protection of DC microgrids, Electric Power Systems Research, 228 (2024) 110010.

[13] M. Čuljak, H. Pandžić, J. Havelka, Mathematical Morphology-Based Fault Detection in Radial DC Microgrids Considering Fault Current from VSC, IEEE Transactions on Smart Grid, (2022).

[14] S.A. Hosseini, S.H.H. Sadeghi, A. Nasiri, Decentralized adaptive protection coordination based on agents social activities for microgrids with topological and operational uncertainties, IEEE Transactions on Industry Applications, 57(1) (2020) 702-713.

[15] W. Javed, D. Chen, I. Kucukdemiral, Fault identifiability and pseudo-data-driven fault localization in a DC microgrid, International Journal of Electrical Power & Energy Systems, 148 (2023) 108944.

[16] M. Sharanya, M.M. Devi, M. Geethanjali, Fault Detection and Location in DC Microgrid, in: 2018 National Power Engineering Conference (NPEC), 2018, pp. 1-7.

[17] J. Yang, J.E. Fletcher, J. O'Reilly, Multiterminal DC wind farm collection grid internal fault analysis and protection design, IEEE Transactions on Power Delivery, 25(4) (2010) 2308-2318.

[18] M.E. Baran, N.R. Mahajan, Overcurrent protection on voltage-source-converter-based multiterminal DC distribution systems, IEEE Transactions on Power Delivery, 22(1) (2006) 406-412.

[19] S.K. Prince, S. Affijulla, G. Panda, Fault detection in IEEE 9-bus DC microgrid system using differential current method, in: 2020 3rd International Conference on Energy, Power and Environment: Towards Clean Energy Technologies, IEEE, 2021, pp. 1-6.

[20] S.D. Fletcher, P.J. Norman, K. Fong, S.J. Galloway, G.M. Burt, High-speed differential protection for smart DC distribution systems, IEEE Transactions on Smart Grid, 5(5) (2014) 2610-2617.

[21] A. Meghwani, S.C. Srivastava, S. Chakrabarti, A Non-unit Protection Scheme for DC Microgrid Based on Local Measurements, IEEE Transactions on Power Delivery, 32(1) (2017) 172-181.

[22] P. Chauhan, C. Gupta, M. Tripathy, High speed fault detection and localization scheme for low voltage DC microgrid, International Journal of Electrical Power & Energy Systems, 146 (2023) 108712.

[23] Z. Li, H. Sui, R. Zhang, G. Wang, H. Cai, Short-circuit fault detection scheme for DC microgrids on offshore platforms, Journal of Power Electronics, 23(5) (2023) 839-849.

[24] A.A. Emhemed, K. Fong, S. Fletcher, G.M. Burt, Validation of fast and selective protection scheme for an LVDC distribution network, IEEE Transactions on Power Delivery, 32(3) (2016) 1432-1440.

[25] R. Mohanty, S. Sahoo, A.K. Pradhan, F. Blaabjerg, A Cosine Similarity-Based Centralized Protection Scheme for dc Microgrids, IEEE Journal of Emerging and Selected Topics in Power Electronics, 9(5) (2021) 5646-5656.

[26] G. Madingou, M. Zarghami, M. Vaziri, Fault detection and isolation in a DC microgrid using a central processing unit, in: 2015 IEEE Power & Energy Society Innovative Smart Grid Technologies Conference (ISGT), IEEE, 2015, pp. 1-5.

[27] Y. Bai, A. Rajapakse, Fault detection and localization in a ring bus DC microgrid using current derivatives, in: 2020 IEEE Canadian Conference on Electrical and Computer Engineering (CCECE), IEEE, 2020, pp. 1-6.

[28] A. Meghwani, S. Chakrabarti, S. Srivastava, A fast scheme for fault detection in DC microgrid based on voltage prediction, in: 2016 National Power Systems Conference (NPSC), IEEE, 2016, pp. 1-6.

[29] L. Kong, H. Nian, Fault detection and location method for mesh-type DC microgrid using pearson correlation coefficient, IEEE Transactions on Power Delivery, 36(3) (2020) 1428-1439.

[30] G.K. Rao, P. Jena, Fault detection in DC microgrid based on the resistance estimation, IEEE Systems Journal, 16(1) (2021) 1009-1020.

[31] D. Spoor, J.G. Zhu, Improved single-ended traveling-wave fault-location algorithm based on experience with conventional substation transducers, IEEE Transactions on Power Delivery, 21(3) (2006) 1714-1720.

[32] C. Li, P. Rakhra, P. Norman, P. Niewczas, G. Burt, P. Clarkson, Modulated low fault-energy protection scheme for DC smart grids, IEEE Transactions on Smart Grid, 11(1) (2019) 84-94.

[33] R.M. May, Simple mathematical models with very complicated dynamics, in: The Theory of Chaotic Attractors, Springer, 2004, pp. 85-93.

[34] M.J. Feigenbaum, The universal metric properties of nonlinear transformations, Journal of Statistical Physics, 21(6) (1979) 669-706.

[35] B. Taheri, A. Shahhoseini, Direct current (DC) microgrid control in the presence of electrical vehicle/photovoltaic (EV/PV) systems and hybrid energy storage systems: A Case study of grounding and protection issue, IET Generation, Transmission & Distribution, (2023).

[36] LT/HT Power & Control Cables.

[37] A. Sistani, S.A. Hosseini, V.S. Sadeghi, B. Taheri, Fault Detection in a Single-Bus DC Microgrid Connected to EV/PV Systems and Hybrid Energy Storage Using the DMD-IF Method, Sustainability, 15(23) (2023) 16269.

[38] L. Shen, Q. Cheng, Y. Cheng, L. Wei, Y. Wang, Hierarchical control of DC micro-grid for photovoltaic EV charging station based on flywheel and battery energy storage system, Electric power systems research, 179 (2020) 106079.

[39] A.M. Harb, I. Batarseh, L.M. Mili, M.A. Zohdy, Bifurcation and chaos theory in electrical power systems: analysis and control, in, Hindawi, 2012.

[40] S.H. Kellert, In the Wake of Chaos: Unpredictable Order in Dynamical Systems, University of Chicago Press, 1993.

[41] P. Sakarung, S. Chatratana, Nonmember, Application of PSCAD/EMTDC and Chaos Theory to Power System Ferroresonance Analysis, (2005).

[42] N.K. Pareek, V. Patidar, K. Sud, Discrete chaotic cryptography using external key, Physics Letters A, 309(1-2) (2003) 75-82.

[43] S. Salehimehr, B. Taheri, F. Razavi, M. Parpaei, M. Faghihlou, A new power swing detection method based on chaos theory, Electrical Engineering, 102(2) (2020) 663-681.

[44] D.L. Gerber, O.A. Ghatpande, M. Nazir, W.G.B. Heredia, W. Feng, R.E. Brown, Energy and power quality measurement for electrical distribution in AC and DC microgrid buildings, Applied Energy, 308 (2022) 118308.

[45] B. Taheri, M. Sedighizadeh, Detection of power swing and prevention of mal-operation of distance relay using compressed sensing theory, IET Generation, Transmission & Distribution, 14(23) (2020) 5558-5570.

[46] M. Mola, A. Afshar, N. Meskin, M. Karrari, Distributed Fast Fault Detection in DC Microgrids, IEEE Systems Journal, 16(1) (2022) 440-451.

[47] N.K. Sharma, S.R. Samantaray, C.N. Bhende, VMD-enabled current-based fast fault detection scheme for DC microgrid, IEEE Systems Journal, 16(1) (2021) 933-944.

[48] Y. Yang, C. Huang, D. Zhou, Y. Li, Fault detection and location in multi-terminal DC microgrid based on local measurement, Electric Power Systems Research, 194 (2021) 107047.

[49] R. Bhargav, B.R. Bhalja, C.P. Gupta, Novel fault detection and localization algorithm for low-voltage DC microgrid, IEEE Transactions on Industrial Informatics, 16(7) (2019) 4498-4511.

[50] M. Monadi, C. Gavriluta, A. Luna, J.I. Candela, P. Rodriguez, Centralized Protection Strategy for Medium Voltage DC Microgrids, IEEE Transactions on Power Delivery, 32(1) (2017) 430-440.

[51] S. Dhar, R.K. Patnaik, P. Dash, Fault detection and location of photovoltaic based DC microgrid using differential protection strategy, IEEE Transactions on Smart Grid, 9(5) (2017) 4303-4312.

HOW TO CITE THIS ARTICLE

A. Sistani, S. A. Hosseini, V. S. Sadeghi, B. Taheri, Providing a fault detection method for the occurrence of faults in DC microgrids, distributed generations, and electrical vehicles, AUT J Electr Eng, 56(2) (2024) 325-342.

DOI: 10.22060/eej.2024.22866.5565